

# Diffusion for Natural Image Matting

Yihan Hu<sup>1</sup>, Yiheng Lin<sup>1</sup>, Wei Wang<sup>1</sup>, Yao Zhao<sup>1</sup>, Yunchao Wei<sup>1,†</sup>, Humphrey Shi<sup>2,†</sup>

<sup>1</sup> Institute of Information Science, Beijing Jiaotong University, <sup>2</sup> Georgia Tech & Picsart AI Research (PAIR)

<https://github.com/YihanHu-2022/DiffMatte>

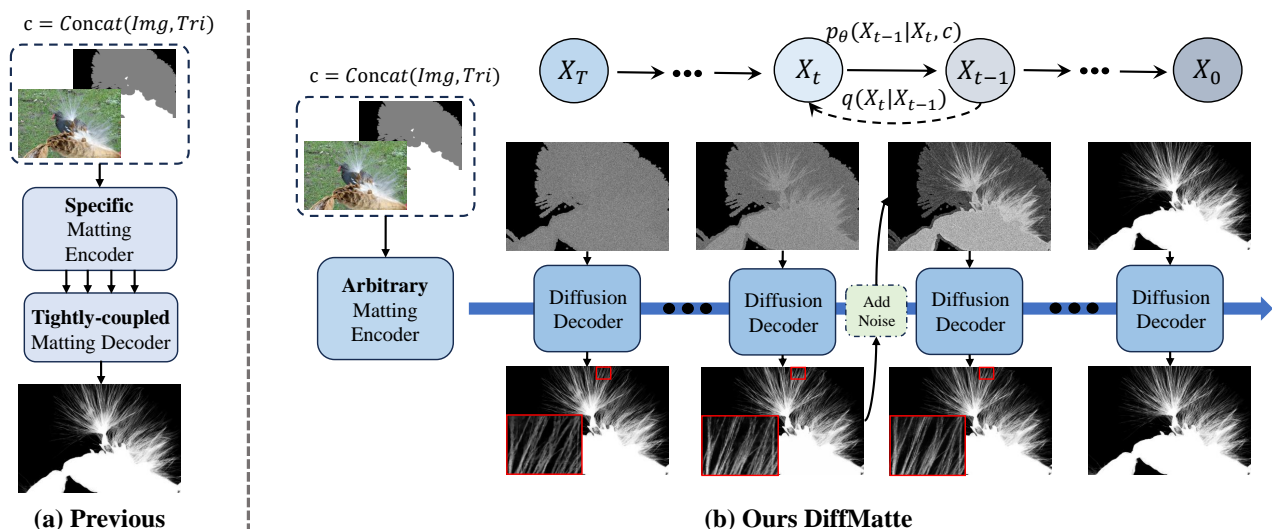


Figure 1. DiffMatte introduces the diffusion process to solve the natural image matting problem. By iteratively correcting the prediction, our method obtains state-of-the-art matting accuracy. DiffMatte can be embedded into arbitrary matting encoders, which makes its application scenarios more flexible and versatile.

## Abstract

We aim to leverage diffusion to address the challenging image matting task. However, the presence of high computational overhead and the inconsistency of noise sampling between the training and inference processes pose significant obstacles to achieving this goal. In this paper, we present DiffMatte, a solution designed to effectively overcome these challenges. First, DiffMatte decouples the decoder from the intricately coupled matting network design, involving only one lightweight decoder in the iterations of the diffusion process. With such a strategy, DiffMatte mitigates the growth of computational overhead as the number of samples increases. Second, we employ a self-aligned training strategy with uniform time intervals, ensuring a consistent noise sampling between training and inference across the entire time domain. Our DiffMatte is designed with flexibility in mind and can seamlessly integrate into various modern matting architectures. Extensive experimental results demonstrate that DiffMatte not only reaches the state-of-the-art level on the Composition-1k test set, sur-

passing the best methods in the past by 5% and 15% in the SAD metric and MSE metric respectively, but also show stronger generalization ability in other benchmarks.

## 1. Introduction

Natural image matting is an important task in computer vision, serving the purpose of isolating foreground objects from their backgrounds. Mathematically, a natural image can be expressed as a linear combination of the foreground  $F \in \mathbb{R}^{H \times W \times C}$ , background  $B \in \mathbb{R}^{H \times W \times C}$ , and the alpha matte  $\alpha \in \mathbb{R}^{H \times W}$ , described as:

$$I_i = \alpha_i F_i + (1 - \alpha_i) B_i, \quad \alpha \in [0, 1], \quad (1)$$

where  $i \in [0, HW]$  represents the index of the pixel in the image,  $H, W, C$  denote height, width, and the number of channels (3 for a color image) respectively. Since the foreground color  $F_i$ , the background color  $B_i$ , and the alpha value  $\alpha$  are left unknown, solving for alpha matte is a highly ill-posed problem. To tackle this, deep neural networks [31, 55, 75, 80] have been widely applied to extract the foreground using a manually labeled trimap as guidance.

<sup>†</sup>Corresponding authors.

The main challenge of deep learning-based matting solutions is how to understand the high-level context knowledge and capture the low-level texture information simultaneously. However, mainstream approaches often focus on either using pre-trained backbones [13, 60, 83] or well-designed modules [12, 46, 74] to enhance the model’s utilization of context information, ignoring the role played by low-level features. This often leads to failures in cases with high and dense uncertainty.

Recently, diffusion probabilistic models [29, 70, 71] have emerged and shown great potential for application and research value with high-fidelity and fine-grained generation [16, 58]. Due to the unique iterative diffusion process, we note that diffusion-generative methods naturally excel in modeling highly complex data distributions and generating realistic texture details. These methods obtain the training samples by adding noise to the clean data, which is used to train the denoising ability of the diffusion model and obtain the prediction results by gradually denoising the signal during the inference. As shown in Figure ?? We believe such an iterative diffusion process of destroying and reconstructing can effectively perceive texture details, which is highly suitable for addressing the matting task.

However, to the best of our knowledge, no pioneer art has successfully adapted the diffusion process to matting models. We believe that this is due to two reasons. First, high computational overhead. Existing matting models, in order to take into account the context knowledge and texture feature, usually adopt a tightly coupled UNet-like design while receiving original-sized images in the inference. This difficulty will be further exacerbated by the direct introduction of such a matting model into the diffusion process. Second, inconsistent noise sampling between the training and inference processes. During training, diffusion involves consistently introducing noise to the target and recovering it through denoising. For the matting problem, noise adoption naturally occurs by utilizing manually annotated alpha matte during training and predicted alpha matte during inference. However, owing to the intricate nature of alpha matte, noise sampling from the predicted alpha matte is often significantly different from the sampled noise during the training phase. This discrepancy renders the trained model unsuitable for inference.

To address the challenges that arise when adapting the diffusion process to matting models, we propose the DiffMatte in this paper. Specifically, to reduce the high computational overhead, DiffMatte decouples the image encoder and decoder. Unlike past one-piece matting predictors, decoder  $\mathcal{D}$  only receives the top-level features of backbone encoder  $\mathcal{B}$  without shortcut connections. During the reverse process of inference, only the lightweight  $\mathcal{D}$  performs iteratively, and  $\mathcal{B}$  acts only once to generate high-dimensional context knowledge, which brings the benefit of a signifi-

cant reduction in computational overhead. Besides, to mitigate the performance decay caused by data discrepancy, DiffMatte includes an additional diffusion step in a single training iteration to replace ground truth alpha matte with a predicted one, reducing the discrepancy in distribution between training and inference. Considering the accumulation of errors across multiple time steps, we propose a self-aligned strategy with uniform time intervals, which achieves uniform alignment of the data distribution across the time domain and brings about stable performance enhancement with the timestep increase. With these two improvements, we successfully migrated the diffusion process to address the challenging matting problem.

Compared to past matting methods, our DiffMatte exhibits two appealing properties: (1) *Encoder conversion*. Our approach refines matting prediction by focusing on the low-level feature of the alpha matte, and our approach decouples the matting decoder for the diffusion process, so we can adapt our approach to a variety of encoders designed for matting and bring about improvements in the quality of matting. (2) *Iterative refinement*. Benefiting from the iterative denoising nature of the diffusion process and our training strategy, DiffMatte is able to iteratively optimize the quality of the alpha matte using shared parameters, with slow growth in computational overheads. When adapted to various matting encoders, DiffMatte outperforms the respective baseline methods on Composition-1k, with the adaptation using ViT-B as the encoder outperforming the previous best method by 5% on the SAD metric. In addition, DiffMatte also obtains higher accuracy when generalizing to the Distinctions-646 and Semantic Image Matting test sets, demonstrating the superiority of our method.

## 2. Related Work

**Natural Image Matting.** Traditional methods are mainly divided into sampling-based [11, 20, 25, 69, 78] and propagation-based methods [5, 26, 41–43, 73], according to the way they make use of color features. These approaches lack the use of context and prone to producing artifacts. Benefiting from the rapid development of deep learning, learning-based methods can access high-level semantic information with the help of neural networks. [12, 46, 50, 51] design learnable modules to exploit contextual knowledge, and [13, 19, 60, 83, 85] introduces stronger backbones [17, 27, 53, 79] to improve matting accuracy. These methods have made significant progress, but lack exploration of low-level texture features. This leads to matting models relying on shortcut connections to provide low-level features in the one-piece UNet like structure. In contrast to the above, [83] proposes a decoder decoupled architecture to utilize a non-hierarchical backbone network ViT, indicating the unnecessary of previous coupled network design. [44, 84] incorporate [37] to extend matting to any instances.



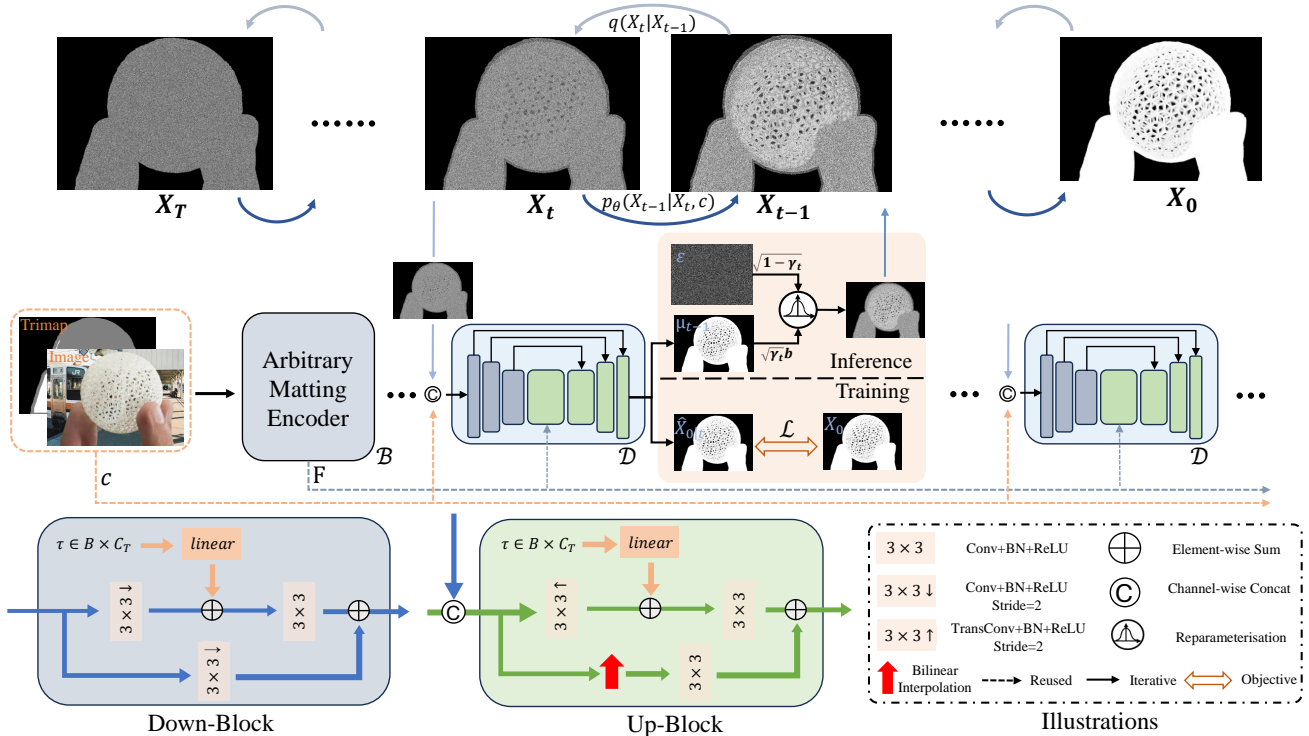


Figure 2. **The proposed DiffMatte Framework.** Our diffusion model can be easily adapted to arbitrary matting encoders. The encoder can be run only once during the diffusion process, and the prediction is continuously refined by iteratively calling the diffusion decoder.

**Diffusion Models.** Diffusion models have achieved significant breakthroughs in various modal generation tasks, owing to their delicate denoising processes. Denoising diffusion probabilistic models (DDPM) [29] accomplishes the inverse diffusion process by training a noise predictor for fine-grained image generation. Denoising diffusion implicit models (DDIM) [70] use non-Markovian processes to speed up sampling. After some successful attempts [57, 63] to fuse textual information, a group of generative large models [59, 62] have achieved surprising results with wide applications in image editing [21, 52, 81]. Diffusion models have also been studied for the generation of a wide range of modalities, including video [28, 30, 35, 77], audio [33, 38, 39], biomedical [68, 76], text [22, 45] and general multimodal frameworks [2, 82].

**Diffusion models for vision tasks.** Diffusion models have attracted extensive research interest due to the success of diffusion modeling in the generative field. Since the pioneering work [1] introduced diffusion methods to solve image segmentation, several follow-ups use diffusion to attempt their respective tasks. [6] formulates object detection as a denoising process. [67] involves a diffusion pipeline into depth estimation approach. [23], [8], and [40] apply diffusion to instance segmentation, panoptic segmentation, and semantic segmentation respectively, where the diffusion denoising training technique used by Pix2Seq [8] is utilized by DDP [34] to solve diversified dense prediction

tasks. These works have achieved good performance by introducing the diffusion process, but [6, 34, 67] observed that the performance decreases as the number of steps increases, and this phenomenon is exacerbated on dense prediction tasks with high accuracy demand.

## 3. Methodology

### 3.1. Constructing Diffusion Framework for Matting

In this section, we construct the basic pipeline of DiffMatte, which is implemented with the well-established diffusion framework to predict the alpha matte. After completing the training of our diffusion model  $f_\theta$ , given an image with trimap, our method gives a list  $L$ , which records the estimates of  $\hat{X}_{0|t}$  at each time step  $t \in \{1, \dots, T\}$ . At this point, we set the last step estimation as the final result.

**Basics of the Diffusion Methods.** Diffusion models [29, 70, 72] are a class of likelihood-based models that are initially used to perform high-quality image generation. These models achieve modeling of complex data distribution through a diffusion process. Specifically, a forward process and a reverse process are included. The data is noised into standard Gaussian noise in successive  $T$  steps in the forward process, which is formulated as:

$$x_t \sim q(x_t|x_0) = \mathcal{N}(x_t; \sqrt{\bar{\alpha}_t}x_0, (1 - \bar{\alpha}_t)\mathbf{I}) \quad (2)$$

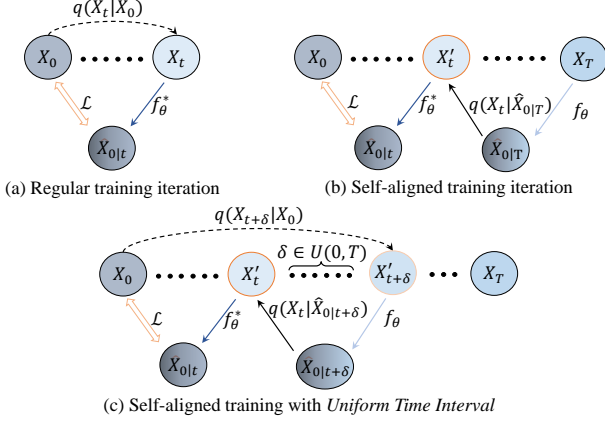


Figure 3. Comparison of different training strategies. In contrast to the strategy proposed by [34], we take into account the accumulation of errors between sampling steps and propose self-aligned strategy with uniform time intervals to align the distribution over the time domain.

where  $\bar{\alpha}_t = \prod_s^t \alpha_s = \prod_s^t (1 - \beta_s)$  and  $\beta_s$  represents the noise variance schedule defined in [29]. Then diffusion model is trained to denoise in the reverse process.

In this work, we aim to solve the natural image matting problem by diffusion modeling. In our setting, the data samples  $X_0$  are ground truth alpha matte  $\mathcal{A}$  that have been normalized to align with the range of noisy data. We train a diffusion matting model conditional on the image and trimap  $c = \text{Concat}(\text{Image}, \text{Trimap})$ , and take  $X_0$  as the expected prediction objective.

**Providing Training Samples through Forward Process.** We adopt the following equation [7] to start forward process:

$$X_t = \sqrt{\gamma_t}(bX_0) + \sqrt{1 - \gamma_t}\epsilon \quad (3)$$

where  $\gamma_t \in (0, 1)$  is a mapping of  $t$  through the noisy function and represents the noise level.  $\epsilon$  is a standard Gaussian noise. In the previous methods, three noisy functions were set up for image generation, namely linear schedule [7, 29], cosine schedule [58] and sigmoid schedule [32], respectively.  $b \in (0, 1]$  indicates the input scaling factor, which increases the noise strength. A smaller  $b$  will bring more destruction of detailed information at the same  $\gamma_t$ , which can be interpreted as an increase to the signal-to-noise ratio (SNR) [7, 8].

In the current phase of training, we sample a single time step  $t$  from a uniform distribution  $U(0, 1)$  following the continuous time training paradigm [9, 36], and noise  $X_0$  to  $X_t$  for an iteration training according to Eq. 3

**Iterative Prediction in Reverse Process.** Given the noisy sample  $X_t$ , the diffusion model obtains the denoised sample  $X_{t-1}$  through estimating  $\mu_{t-1} = \hat{X}_{0|t}$  with trained  $f_\theta$ . After that a sampling technique proposed by DDIM [70] is used to sample  $X_{t-1}$ , which can be defined as:

$$X_{t-1} \sim \mathcal{N}(X_{t-1}; \sqrt{\gamma_{t-1}}\mu_{t-1}, (1 - \gamma_{t-1})\mathbf{I}) \quad (4)$$

Time Steps	1	5	10
GCA [46]	2.09	10.45	20.90
DiffMatte-Res34	1.12	4.56	8.86
ViTMatte-S [83]	1.69	8.45	16.90
DiffMatte-ViTS	2.08	5.36	9.46

Table 1. Computational overhead growth with sample step increase. We use an image with a resolution of 2048x2048 as input, with computational overhead in TFLOPs. DiffMatte uses a lightweight diffusion decoder and the backbone is not involved in the diffusion process, so the computational overhead grows more slowly in iterations compared to other matting methods.

Combining the estimation of  $\mu_{t-1}$  and DDIM sampling, we get one iteration of the reverse process:

$$p_\theta(X_{t-1}|X_t, c) = \mathcal{N}(X_{t-1}; \sqrt{\gamma_{t-1}}f_\theta(X_t, t, c), (1 - \gamma_{t-1})\mathbf{I}) \quad (5)$$

The complete reverse process starts with a standard Gaussian noise  $X_T$  and passes through a preset  $T$ -step iteration to get the final estimation  $\hat{X}_0$ . During inference, as the time step goes from  $T$  to 0, the value of  $\gamma_t$  is mapped from 1 to 0 via the noisy function. Thus  $X_T \sim \mathcal{N}(0, I)$ , which is consistent with  $\epsilon$  at the beginning time step  $T$ .

### 3.2. DiffMatte

**Decoupled texture decoder for efficient diffusion process.** The network designed for the matting task is usually a tightly coupled one-piece structure [12, 13, 31, 46], joining this to the iterative diffusion process without modification leads to excessive computational overhead. Inspired by structural designs of [83] and [34], we decouple  $f_\theta$  into separate context encoder  $\mathcal{B}$  and texture decoder  $\mathcal{D}$ , the connection between the two is limited to the top-level context feature provided by  $\mathcal{B}$ . We implement the diffusion model  $f_\theta$  as:

$$F = \mathcal{B}(c) \quad (6)$$

$$f_\theta(X_t, t, c) = \mathcal{D}(\text{cat}(X_t, c), t, F) = \mu_{t-1}$$

As shown in Figure 2,  $\mathcal{B}$  encodes the image with the information of trimap to get the context knowledge  $F$ , which will be reused in the reverse process.  $\mathcal{D}$  is iteratively performed in the diffusion process, and its lightweight structure prevents excessive computational overheads. We construct the decoupled diffusion decoder  $\mathcal{D}$  with stacked down-blocks and up-blocks. One up-block is used to receive and adapt contextual knowledge from  $\mathcal{B}$ . The rest of the up-block and down-block are paired with each other and improve the extraction of textural information through feature concatenation. In this way, the diffusion process can be smoothly implemented using the lightweight diffusion decoder, and the heavy encoder only propagates once to avoid

---

**Algorithm 1: DiffMatte Training**

---

```
def train(cond, pha, flag, b):  
    """ cond: [B, 4, H, W], pha: [B, 1, H, W] """  
    """ flag: self-align entry, b: input scale """  
    feat = mat_encoder(cond) # encode condition  
    pha = (pha * 2) - 1 # normalzie  
    # forward process  
    t, eps = uniform(0, 1), normal(0, 1)  
    if flag == True:  
        Xt = self_align(t, eps) # get aligned sample  
    else:  
        gamma = noisy_func(t)  
        Xt = sqrt(gamma) * pha + sqrt(1-gamma) * eps  
    # predict and backward  
    X0 = diff_decoder(Xt, cond, feat, t)  
    X0 = (X0 + 1) / 2  
    loss = Losses(X0, pha)  
    return loss
```

---

computational redundancy. Our diffusion decoder can be adapted to various matting encoders by varying the number of down-block vs. up-block pairs, as described in the construction details in the Supplementary Material. Also, the hyperparameter  $N_d$ , which controls the number of block channels, can be varied to meet accuracy or computational overhead requirements. As shown in Table 1, with this lightweight design, DiffMatte saves 12.04 TFLOPs (57.6%) computational overhead over GCA when sampling 10 steps with ResNet34 encoder, and 7.44 TFLOPs (44.0%) computational overhead over ViTMatte with ViT-S encoder.

**Self-aligned strategy with uniform time intervals for consistent noise sampling.** We analyze  $L$  and observe that the accuracy of DiffMatte’s estimations for  $X_0$  decreases with growing time steps (the evidence is displayed in Figure 4 (b)). This phenomenon has been reported on numerous perceptual methods that introduce diffusion processes [6, 34, 67]. Among them, DDP [34] proposes a self-aligned strategy to align the data distribution of training and inference by replacing the training target with model predictions. We attribute this phenomenon to the error accumulation and amplification in the diffusion iteration process caused by inconsistencies in the training and inference noise samples. The approach proposed by [34] is limited as the ignorance of the accumulation of deviation that occurs during multiple-step sampling, which is even more pronounced in matting tasks.

We propose a more refined strategy that effectively corrects this distribution variance by converting sampling targets to time intervals, obtaining a self-aligned strategy with Uniform Time Intervals (UTI). As shown in Figure 3, we sample a time interval  $\delta \in U(0, T)$ , which acts on the training time step  $t \in U(0, T - \delta)$  to obtain  $\hat{t} = t + \delta$ . In the subsequent procedures, we use an additional forward process  $q(X_{\hat{t}}|X_0)$  to calculate the previous step noise

---

**Algorithm 2: DiffMatte Inference**

---

```
def inference(cond, T, b):  
    """ cond: [B, 4, H, W], T: sampling steps """  
    """ b: input scale """  
    feat = mat_encoder(cond) # encode condition  
    Xt = normal(0, 1) # noisy map of [B, 1, H, W]  
    time_pairs = sample_timesteps(T)  
    # reverse process  
    for t, t_next in time_pairs:  
        gamma, gamma_next = noisy_func(t, t_next)  
        # normalize X_t by variance  
        Xt = Xt / std(Xt)  
        # predict X0  
        X0 = diff_decoder(Xt, cond, feat, t)  
        X0 = (X0 * 2) - 1 # normalize  
        Xt = DDIM(X0, gamma, gamma_next, b)  
    Xpred = Xt / b # rescaling  
    return [Xpred + 1] / 2 # denormalize
```

---

sample instead of using white noise like [34]. After that, we obtain the estimation  $\hat{X}_{0|t+\delta}$  of the current sample  $X'_{t+\delta}$  over  $X_0$  by a frozen diffusion model  $f_\theta$ . After replacing  $X_0$  with  $\hat{X}_{0|t+\delta}$  we perform a regular training iteration. The use of  $X_{\hat{t}}$  helps the model to complete the alignment of the data distribution over the entire time domain and mitigate the accumulation of errors. Once  $\delta$  takes the value of 0, our method reverts to regular training, while when  $\delta$  takes the value of  $T - t$  it becomes the case used by [34]. We add our UTI self-aligned strategy after  $f_\theta$  is well-trained to prevent serious errors in estimation  $\hat{X}_{0|t}$  from causing the training failure.

### 3.3. Training and Inference.

Our training and inference algorithms are shown in Algorithm 1 and Algorithm 2. Our approach requires a selected noise schedule as well as input scaling, both of which parameterize the corresponding noise distribution, leading to different diffusion processes. DiffMatte involves the timing of the start of the UTI self-aligned strategy during training. We train to the 90th epoch to add it and continue until the end of training. At training time our  $f_\theta$  is supervised with the task-specific losses following the common practices [6, 8, 34]:

$$\mathcal{L} = E_{t \sim U(1, T), X_t \sim q(X_t | X_0, \mathbf{I})} \mathcal{L}_{mat}(f_\theta(X_t, t, c), X_0) \quad (7)$$

specifically using the combined matting loss with separate  $l_1$  loss [83],  $l_2$  loss, laplacian loss [31], and gradient penalty loss. We end up with the following objective:

$$\mathcal{L}_{mat} = \mathcal{L}_{sp} l_1 + \mathcal{L}_{l_2} + \mathcal{L}_{lap} + \mathcal{L}_{grad} \quad (8)$$

Thanks to continuous-time training, we are free to set the total number of iterations  $T$  during inference. As demonstrated in Figure 4 (a), an increase in the number of sample

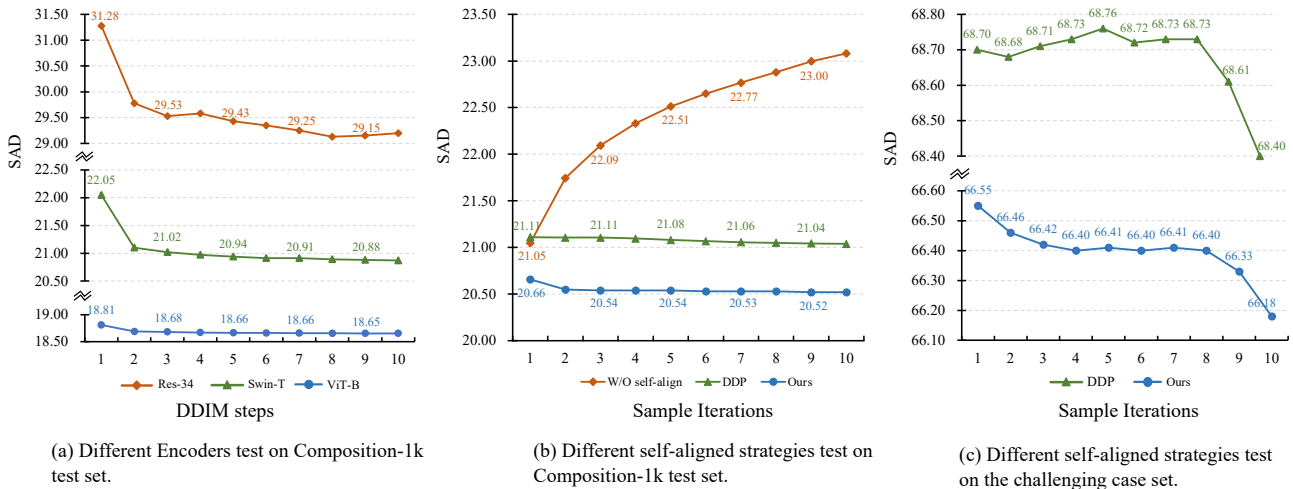


Figure 4. Main Properties of DiffMatte. All experiments are trained on Adobe Image Matting Datasets[80].

steps from 1 to 10 is accompanied by an improvement in the accuracy of the final prediction.

## 4. Experiments

### 4.1. Datasets and Evaluation.

**Adobe Image Matting [80].** This dataset contains 431 unique training foreground images and 50 extra foregrounds for evaluation. The training set was constructed by compositing each foreground with 100 background images from the COCO dataset [49]. Similarly, the validation set named Composition-1k is obtained by compositing 50 test foreground images with 20 background images from VOC2012 [18] to get a total of 1000 test images.

**Distinctions-646 [61].** For the Distinctions-646 (hereinafter referred to as D646) dataset, it provides 50 test foregrounds, which are synthesized with the background in VOC2012 into a test data set containing 1000 images. Since no trimap is provided, we generate trimap by randomly dilating-eroding the ground truth alpha matte. We selected some past methods and re-tested them using the trimaps we generated to ensure fairness.

**Semantic Image Matting [74].** As a complement to the Composition-1k test set, this dataset provided by Semantic Image Matting Dataset (hereafter referred to as SIMD) contains 39 foreground instances of diverse categories. By the time of our writing, SIMD had included a companion trimap generation code, so we used this officially provided trimap for evaluation.

We train our model on the Adobe Image Matting training set and perform inference on all three test sets to validate the matting performance as well as the generalization. We use 4 common metrics to evaluate our DiffMatte: Sum of Absolute Differences (SAD), Mean Square Error (MSE), Gradient loss (Grad), and Connectivity loss (Conn). A lower value indicates better alpha matte quality.

Methods	SAD	MSE( $10^3$ )	Grad	Conn
DIM [80]	50.4	14.0	31.0	50.8
IndexNet [54]	45.8	13.0	25.9	43.7
SampleNet [75]	40.4	9.9	-	-
Context-Aware [31]	35.8	8.2	17.3	33.2
A <sup>2</sup> U [12]	32.2	8.2	16.4	29.3
MG <sup>†</sup> [86]	31.5	6.8	13.5	27.3
SIM [74]	28.0	5.8	10.8	24.8
FBA [19]	25.8	5.2	10.6	20.8
TransMatting [3]	24.96	4.58	9.72	20.16
RMat [13]	22.87	3.9	7.74	17.84
GCA [46]	35.3	9.1	16.9	32.5
DiffMatte-Res34 (S1)	31.28	6.38	11.60	28.07
DiffMatte-Res34 (S10)	<b>29.20</b>	<b>6.04</b>	<b>11.31</b>	<b>25.48</b>
Matteformer [60]	23.80	4.03	8.68	18.90
DiffMatte-SwinT (S1)	22.05	3.54	6.67	17.03
DiffMatte-SwinT (S10)	<b>20.87</b>	<b>3.23</b>	<b>6.37</b>	<b>15.84</b>
ViTMatte-S [83]	21.46	3.3	7.24	16.21
DiffMatte-ViT-S (S1)	20.61	3.08	7.14	14.98
DiffMatte-ViT-S (S10)	<b>20.52</b>	<b>3.06</b>	<b>7.05</b>	<b>14.85</b>
ViTMatte-B [83]	20.33	3.0	6.74	14.78
DiffMatte-ViT-B (S1)	18.84	2.56	5.86	13.23
DiffMatte-ViT-B (S10)	<b>18.63</b>	<b>2.54</b>	<b>5.82</b>	<b>13.10</b>

Table 2. Quantitative results on Composition-1K [80]. † indicates using the foreground area of trimap as guidance. The best results are shown in bold. S1 and S10 denote 1 and 10 DDIM steps.

### 4.2. Main Properties

**Encoder Conversion.** DiffMatte can pair with various matting-specific encoders with only a few modifications to the diffusion decoder. We use ResNet-34 [27] modified by [46], the Swin-Tiny [53] adaption proposed by [60], and the ViT-B [17] adaption proposed by [83] as matting encoders to test on the Composition-1k with different DDIM sam-



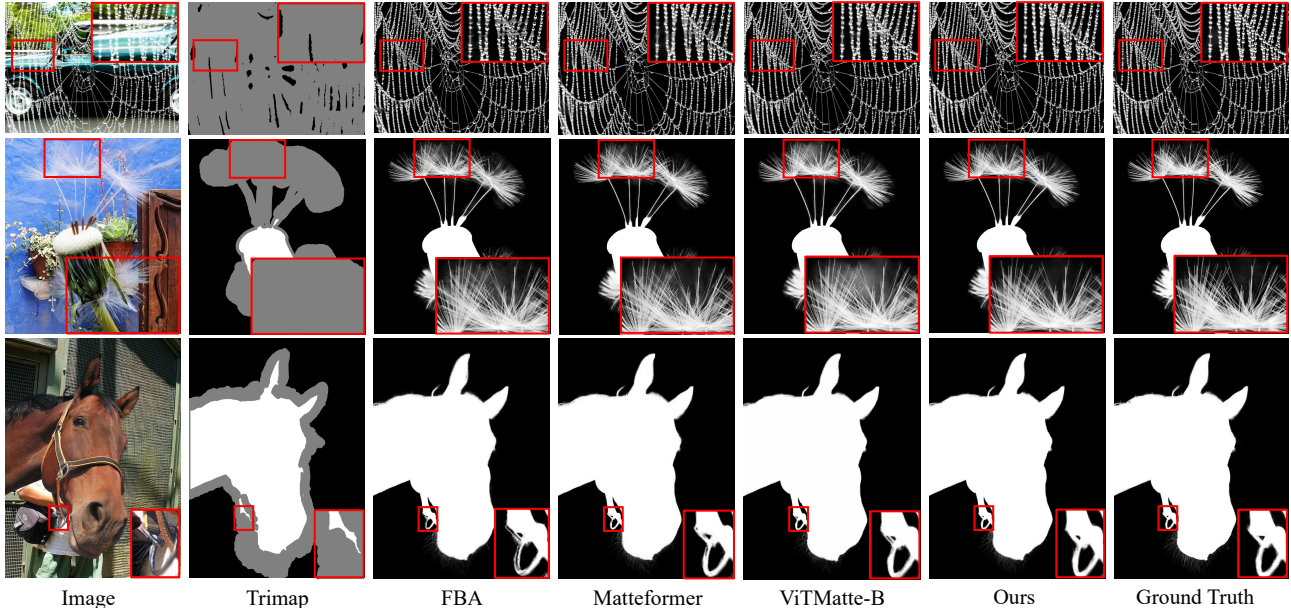


Figure 5. Qualitative results compared with previous SOTA methods on Composition-1k. Best viewed by zooming in.

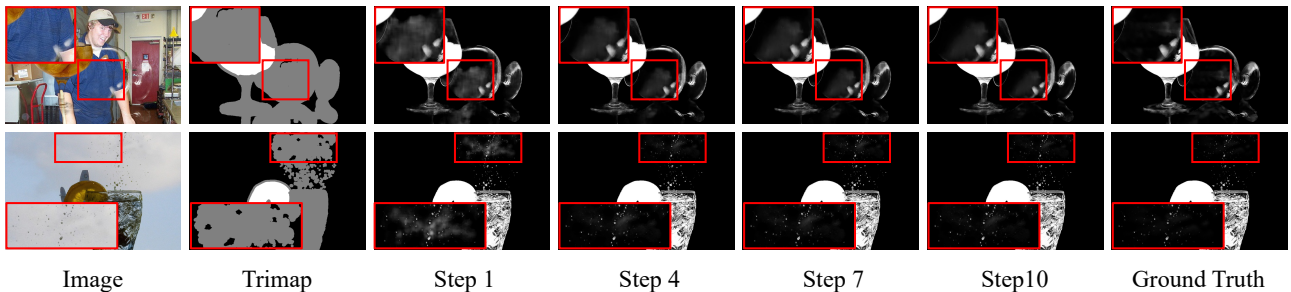


Figure 6. Visualizing the Inference Trajectory: Depicting the predicted alpha matte at different iterations while employing DDIM with 10 sampling steps.

pling steps. Figure 4 (a), illustrates that integrating more robust encoders not only boosts overall performance but also marginally increases matting accuracy with the escalation in the total number of sampling steps. Unlike previous methods constrained to specific matting encoders, DiffMatte offers greater versatility, seamlessly integrating into diverse architectural frameworks.

**Iterative Refinement.** For a given number of sampling steps  $T = 10$ , we observe the accuracy of the estimation of  $X_0$  in  $L$ . As shown in Figure 4 (b), it can be observed that in the absence of any kind of self-aligned strategy, the model performance dramatically decays as the time steps increase. This suggests that the sample drift phenomenon introduced in [34] severely affects the performance of diffusion processes migrated to matting models. Compared with the strategy proposed in DDP, our approach leads to higher precision and reaches the top earlier. The training strategy proposed by DDP requires more than ten steps to converge, while our method is within five steps, and the accuracy is better (+0.52 in SAD). We further compare our

strategy with DDP proposed on the top 20% of the challenging case set in Composition-1k, and as shown in Figure 4 (c), our approach has a more consistent refinement and larger growth (+0.37 vs. +0.30), demonstrating the effectiveness of our method.

### 4.3. Natural Image Matting Benchmarks

**Results on Composition-1k.** The quantitative and qualitative results on Composition-1k are shown in Table 2. When using the ViT-B encoder, DiffMatte only performs one sampling step and improves the SAD metric by 1.49 (+7.3%) and the MSE metric by 0.44 (+14.7%) compared with ViT-Matte. When sampling for ten steps, the SAD and MSE were further improved by 0.21 and 0.04 respectively. The results indicate that our method outperforms others by a large margin and achieves *state-of-the-art* (SOTA) performance. The performance improvements become more noticeable when using Swin Tiny and ResNet-34.

**Generalization on D646 and SIMD.** The quantitative results on D646 and SIMD test sets are shown in Table 3.

Dataset Method	Distinctions-646				Semantic Image Matting Dataset				Params
	SAD	MSE	Grad	Conn	SAD	MSE	Grad	Conn	
GCA [46]	35.33	18.4	28.78	34.29	68.23	25.74	33.19	67.67	25.3M
DiffMatte-Res34 (S1)	31.53	11.87	17.52	30.86	51.49	14.10	18.32	48.70	23.9M
DiffMatte-Res34 (S10)	<b>29.38</b>	<b>11.31</b>	<b>16.19</b>	<b>28.26</b>	<b>47.75</b>	<b>14.10</b>	<b>17.19</b>	<b>44.53</b>	
Matteformer [60]	23.90	8.16	12.65	<b>18.90</b>	29.66	5.91	12.52	24.19	48.8M
DiffMatte-SwinT (S1)	23.46	6.71	10.20	21.23	30.26	5.64	9.45	24.64	38.8M
DiffMatte-SwinT (S10)	<b>23.17</b>	<b>6.58</b>	<b>10.04</b>	20.03	<b>27.51</b>	<b>5.20</b>	<b>9.12</b>	<b>22.04</b>	
ViTMatte-S [83]	23.18	7.14	13.97	19.65	27.96	5.02	10.68	22.38	25.8M
DiffMatte-ViT-S (S1)	<b>22.56</b>	<b>7.09</b>	13.21	<b>19.23</b>	27.55	4.78	<b>10.26</b>	21.24	29.0M
DiffMatte-ViT-S (S10)	22.96	7.22	<b>13.06</b>	19.66	<b>27.38</b>	<b>4.71</b>	10.31	<b>21.03</b>	
ViTMatte-B [83]	20.36	5.58	9.34	17.19	27.15	5.45	9.67	21.51	96.7M
DiffMatte-ViT-B (S1)	<b>19.07</b>	<b>5.23</b>	9.26	<b>15.99</b>	26.83	4.92	8.26	20.72	101.4M
DiffMatte-ViT-B (S10)	19.19	5.34	<b>9.26</b>	16.17	<b>25.60</b>	<b>4.69</b>	<b>8.20</b>	<b>19.84</b>	

Table 3. Quantitative results on D646 [61] and SIMD [74]. All methods are trained only on the Adobe Image Matting training set. The best results are shown in bold. S1 and S10 denote 1 and 10 DDIM steps.

Noise Schedule	SAD	MSE	Input Scaling	SAD	MSE	$N_d$	SAD	MSE	Params	TFLOPs
sigmoid	21.46	3.31	0.05	21.0	3.32	16	21.63	3.55	1.9M	0.2
cosine	21.58	3.35	0.1	21.30	3.24	24	21.23	3.27	3.4M	0.5
<b>linear</b>	<b>20.60</b>	<b>3.15</b>	<b>0.2</b>	<b>20.52</b>	<b>3.06</b>	32	20.52	3.06	5.3M	0.8
			0.5	20.88	3.24	48	20.29	3.05	10.0M	1.8
			1.0	22.19	3.75					

(a) **Noise Schedule.** We find linear schedule works best for matting task.

(b) **Input Scaling.** The best input scaling factor is 0.2.

(c) **Diffusion Decoder Channels.**  $N_d$  set to 32 can best balance the parameters and computational overhead.

Table 4. **ablation experiments** with ViT-S [83] on Composition-1k test set [80]. We report the performance with 10 DDIM sampling steps in (a), (b), and (c). Default settings are marked in gray.

All compared methods use the officially provided weights trained on the Adobe Image Matting training set to test the generalizability. The results show that DiffMatte outperforms all other selected methods on both D646 and SIMD test sets, indicating the superiority of our method. It is worth noting that DiffMatte based on the ViT backbone shows a trend of performance degradation with increasing time steps on the D646 test set, which we attribute to the fact that on unseen data, the data distribution of training and inference is shifted even more drastically in distance, in the meanwhile the decoder adapted to ViT is more shallow, and therefore lack of adaptive capacity.

#### 4.4. Qualitative Results

**Visualization on Composition-1k.** Figure 7 qualitatively comparing our approach to previous SOTA methods, represents that our method performs better in the perception of fine regions, demonstrating the superiority of our approach.

**Visualizing the Inference Trajectory.** DiffMatte can iteratively refine predictions at each step. Figure 6 shows our two inference trajectories. It can be clearly observed that the errors in prediction are corrected as the number of sampling iterations increases. This ability to correct predictions is not available in past matting methods.

#### 4.5. Ablation Study

We perform ablation experiments on our diffusion training approach on the Composition-1k test set. All models are trained using ViT-S as the matting encoder.

**Noisy function.** We study the effect of the noisy function in Table 4a and observe that the linear schedule is best suited for matting tasks compared to cosine and sigmoid schedules. This conclusion differs from the practice of diffusion methods on generative [7] and other perceptual tasks [34]. This is attributed to the need for fine area guidance, the linear schedule’s relatively stable SNR variation ratio facilitates the model for detail perception.

**Input Scaling.** As shown in Table 4b, we conduct a series of ablations on the input scaling and obtained the optimal scale factor. The model performs worst with a factor of 1.0. We believe that this  $x_t$  is too simple for training the model and leads to inadequate learning. The performance of the model steadily improves as the factor decreases and reaches its best level at 0.2, obtaining an improvement of 1.67 in SAD and 0.71 in MSE. This demonstrates that techniques previously effective on other diffusion perception methods [8, 34] are also effective on the matting task. As the scale factor is further reduced, the performance of the model ap-

pears to degrade. This suggests that too noisy  $x_t$  is detrimental to model training.

**Diffusion Decoder Channels.** As shown in Table 4c, we study the role of the number of decoder channels  $N_d$ . As  $N_d$  increases, the matting accuracy of the model will be improved, but the number of parameters and computational overhead will also increase. We find that when  $N_d$  is set to 32, it has relatively good performance, while the computational overhead is within an acceptable range.

## 5. Conclusion

This paper successfully applies the diffusion method to a natural image matting task through a decoupled decoder and a self-aligned strategy with uniform time intervals. Our method continuously improves predictions during multi-step sampling without introducing excessive computational overhead. We achieve state-of-the-art performance on the Composition-1k benchmark, and the generalization of our method outperforms past methods on the Distinctions-646 and Semantic Image Matting test sets. This reflects that diffusion has great potential for fine-grained segmentation and expansion potential for related tasks.

**Limitations and Future Work.** Our method will reach the performance bottleneck while the sample step increases. This is because the development of matting models is still insufficient to predict alpha matte perfectly. However, if artificial correction methods can be introduced during inference, interactive matting can be achieved. This has significant potential in the field of image editing.

## References

- [1] Tomer Amit, Tal Shaharbany, Eliya Nachmani, and Lior Wolf. Segdiff: Image segmentation with diffusion probabilistic models. *arXiv preprint arXiv:2112.00390*, 2021. 3
- [2] Fan Bao, Shen Nie, Kaiwen Xue, Chongxuan Li, Shi Pu, Yaole Wang, Gang Yue, Yue Cao, Hang Su, and Jun Zhu. One transformer fits all distributions in multi-modal diffusion at scale. *arXiv preprint arXiv:2303.06555*, 2023. 3
- [3] Huanqia Cai, Fanglei Xue, Lele Xu, and Lili Guo. Transmatting: Enhancing transparent objects matting with transformers. In *European Conference on Computer Vision*, pages 253–269. Springer, 2022. 6
- [4] Mathilde Caron, Hugo Touvron, Ishan Misra, Hervé Jégou, Julien Mairal, Piotr Bojanowski, and Armand Joulin. Emerging properties in self-supervised vision transformers. In *Proceedings of the IEEE/CVF international conference on computer vision*, pages 9650–9660, 2021.
- [5] Qifeng Chen, Dingzeyu Li, and Chi-Keung Tang. Knn matting. *IEEE transactions on pattern analysis and machine intelligence*, 35(9):2175–2188, 2013. 2
- [6] Shoufa Chen, Peize Sun, Yibing Song, and Ping Luo. Diffusiondet: Diffusion model for object detection. In *Proceedings of the IEEE/CVF International Conference on Computer Vision*, pages 19830–19843, 2023. 3, 5
- [7] Ting Chen. On the importance of noise scheduling for diffusion models. *arXiv preprint arXiv:2301.10972*, 2023. 4, 8
- [8] Ting Chen, Lala Li, Saurabh Saxena, Geoffrey Hinton, and David J Fleet. A generalist framework for panoptic segmentation of images and videos. In *Proceedings of the IEEE/CVF International Conference on Computer Vision*, pages 909–919, 2023. 3, 4, 5, 8
- [9] Ting Chen, Ruixiang Zhang, and Geoffrey Hinton. Analog bits: Generating discrete data using diffusion models with self-conditioning. *arXiv preprint arXiv:2208.04202*, 2022. 4
- [10] Donghyeon Cho, Yu-Wing Tai, and Inso Kweon. Natural image matting using deep convolutional neural networks. In *Computer Vision—ECCV 2016: 14th European Conference, Amsterdam, The Netherlands, October 11–14, 2016, Proceedings, Part II 14*, pages 626–643. Springer, 2016.
- [11] Yung-Yu Chuang, Brian Curless, David H Salesin, and Richard Szeliski. A bayesian approach to digital matting. In *Proceedings of the 2001 IEEE Computer Society Conference on Computer Vision and Pattern Recognition. CVPR 2001*, volume 2, pages II–II. IEEE, 2001. 2
- [12] Yutong Dai, Hao Lu, and Chunhua Shen. Learning affinity-aware upsampling for deep image matting. In *Proceedings of the IEEE/CVF Conference on Computer Vision and Pattern Recognition*, pages 6841–6850, 2021. 2, 4, 6
- [13] Yutong Dai, Brian Price, He Zhang, and Chunhua Shen. Boosting robustness of image matting with context assembling and strong data augmentation. In *Proceedings of the IEEE/CVF Conference on Computer Vision and Pattern Recognition*, pages 11707–11716, 2022. 2, 4, 6
- [14] Giannis Daras, Yuval Dagan, Alexandros G Dimakis, and Constantinos Daskalakis. Consistent diffusion models: Mitigating sampling drift by learning to be consistent. *arXiv preprint arXiv:2302.09057*, 2023.
- [15] Jia Deng, Wei Dong, Richard Socher, Li-Jia Li, Kai Li, and Li Fei-Fei. Imagenet: A large-scale hierarchical image database. In *2009 IEEE conference on computer vision and pattern recognition*, pages 248–255. Ieee, 2009.
- [16] Prafulla Dhariwal and Alexander Nichol. Diffusion models beat gans on image synthesis. *Advances in neural information processing systems*, 34:8780–8794, 2021. 2
- [17] Alexey Dosovitskiy, Lucas Beyer, Alexander Kolesnikov, Dirk Weissenborn, Xiaohua Zhai, Thomas Unterthiner, Mostafa Dehghani, Matthias Minderer, Georg Heigold, Sylvain Gelly, et al. An image is worth 16x16 words: Transformers for image recognition at scale. *arXiv preprint arXiv:2010.11929*, 2020. 2, 6
- [18] Mark Everingham, Luc Van Gool, Christopher KI Williams, John Winn, and Andrew Zisserman. The pascal visual object classes (voc) challenge. *International journal of computer vision*, 88:303–338, 2010. 6
- [19] Marco Forte and François Pitié.  $f$ ,  $b$ , alpha matting. *arXiv preprint arXiv:2003.07711*, 2020. 2, 6
- [20] Eduardo SL Gastal and Manuel M Oliveira. Shared sampling for real-time alpha matting. In *Computer Graphics Forum*, volume 29, pages 575–584. Wiley Online Library, 2010. 2
- [21] Vidit Goel, Elia Peruzzo, Yifan Jiang, Dejie Xu, Nicu Sebe, Trevor Darrell, Zhangyang Wang, and Humphrey Shi. Pair-diffusion: Object-level image editing with structure-



- and-appearance paired diffusion models. *arXiv preprint arXiv:2303.17546*, 2023. [3](#)
- [22] Shansan Gong, Mukai Li, Jiangtao Feng, Zhiyong Wu, and LingPeng Kong. Diffuseq: Sequence to sequence text generation with diffusion models. *arXiv preprint arXiv:2210.08933*, 2022. [3](#)
- [23] Zhangxuan Gu, Haoxing Chen, Zhuoer Xu, Jun Lan, Changhua Meng, and Weiqiang Wang. Diffusioninst: Diffusion model for instance segmentation. *arXiv preprint arXiv:2212.02773*, 2022. [3](#)
- [24] Kaiming He, Xinlei Chen, Saining Xie, Yanghao Li, Piotr Dollár, and Ross Girshick. Masked autoencoders are scalable vision learners. In *Proceedings of the IEEE/CVF conference on computer vision and pattern recognition*, pages 16000–16009, 2022.
- [25] Kaiming He, Christoph Rhemann, Carsten Rother, Xiaoou Tang, and Jian Sun. A global sampling method for alpha matting. In *CVPR 2011*, pages 2049–2056. Ieee, 2011. [2](#)
- [26] Kaiming He, Jian Sun, and Xiaoou Tang. Fast matting using large kernel matting laplacian matrices. In *2010 IEEE Computer Society Conference on Computer Vision and Pattern Recognition*, pages 2165–2172. IEEE, 2010. [2](#)
- [27] Kaiming He, Xiangyu Zhang, Shaoqing Ren, and Jian Sun. Deep residual learning for image recognition. In *Proceedings of the IEEE conference on computer vision and pattern recognition*, pages 770–778, 2016. [2](#), [6](#)
- [28] Jonathan Ho, William Chan, Chitwan Saharia, Jay Whang, Ruiqi Gao, Alexey Gritsenko, Diederik P Kingma, Ben Poole, Mohammad Norouzi, David J Fleet, et al. Imagen video: High definition video generation with diffusion models. *arXiv preprint arXiv:2210.02303*, 2022. [3](#)
- [29] Jonathan Ho, Ajay Jain, and Pieter Abbeel. Denoising diffusion probabilistic models. *Advances in neural information processing systems*, 33:6840–6851, 2020. [2](#), [3](#), [4](#)
- [30] Wenyi Hong, Ming Ding, Wendi Zheng, Xinghan Liu, and Jie Tang. Cogvideo: Large-scale pretraining for text-to-video generation via transformers. *arXiv preprint arXiv:2205.15868*, 2022. [3](#)
- [31] Qiqi Hou and Feng Liu. Context-aware image matting for simultaneous foreground and alpha estimation. In *Proceedings of the IEEE/CVF International Conference on Computer Vision*, pages 4130–4139, 2019. [1](#), [4](#), [5](#), [6](#)
- [32] Allan Jabri, David Fleet, and Ting Chen. Scalable adaptive computation for iterative generation. *arXiv preprint arXiv:2212.11972*, 2022. [4](#)
- [33] Yujin Jeong, Wonjeong Ryoo, Seunghyun Lee, Dabin Seo, Wonmin Byeon, Sangpil Kim, and Jinkyu Kim. The power of sound (tpos): Audio reactive video generation with stable diffusion. In *Proceedings of the IEEE/CVF International Conference on Computer Vision*, pages 7822–7832, 2023. [3](#)
- [34] Yuanfeng Ji, Zhe Chen, Enze Xie, Lanqing Hong, Xihui Liu, Zhaoqiang Liu, Tong Lu, Zhenguo Li, and Ping Luo. Ddp: Diffusion model for dense visual prediction. *arXiv preprint arXiv:2303.17559*, 2023. [3](#), [4](#), [5](#), [7](#), [8](#)
- [35] Levon Khachatryan, Andranik Movsisyan, Vahram Tadevosyan, Roberto Henschel, Zhangyang Wang, Shant Navasardyan, and Humphrey Shi. Text2video-zero: Text-to-image diffusion models are zero-shot video generators. In *Proceedings of the IEEE/CVF International Conference on Computer Vision (ICCV)*, 2023. [3](#)
- [36] Diederik Kingma, Tim Salimans, Ben Poole, and Jonathan Ho. Variational diffusion models. *Advances in neural information processing systems*, 34:21696–21707, 2021. [4](#)
- [37] Alexander Kirillov, Eric Mintun, Nikhila Ravi, Hanzi Mao, Chloe Rolland, Laura Gustafson, Tete Xiao, Spencer Whitehead, Alexander C Berg, Wan-Yen Lo, et al. Segment anything. *arXiv preprint arXiv:2304.02643*, 2023. [2](#)
- [38] Alexander Kolesnikov, Lucas Beyer, Xiaohua Zhai, Joan Puigcerver, Jessica Yung, Sylvain Gelly, and Neil Houlsby. Big transfer (bit): General visual representation learning. In *Computer Vision–ECCV 2020: 16th European Conference, Glasgow, UK, August 23–28, 2020, Proceedings, Part V 16*, pages 491–507. Springer, 2020. [3](#)
- [39] Zhifeng Kong, Wei Ping, Jiaji Huang, Kexin Zhao, and Bryan Catanzaro. Diffwave: A versatile diffusion model for audio synthesis. *arXiv preprint arXiv:2009.09761*, 2020. [3](#)
- [40] Zeqiang Lai, Yuchen Duan, Jifeng Dai, Ziheng Li, Ying Fu, Hongsheng Li, Yu Qiao, and Wenhai Wang. Denoising diffusion semantic segmentation with mask prior modeling. *arXiv preprint arXiv:2306.01721*, 2023. [3](#)
- [41] Philip Lee and Ying Wu. Nonlocal matting. In *CVPR 2011*, pages 2193–2200. IEEE, 2011. [2](#)
- [42] Anat Levin, Dani Lischinski, and Yair Weiss. A closed-form solution to natural image matting. *IEEE transactions on pattern analysis and machine intelligence*, 30(2):228–242, 2007.
- [43] Anat Levin, Alex Rav-Acha, and Dani Lischinski. Spectral matting. *IEEE transactions on pattern analysis and machine intelligence*, 30(10):1699–1712, 2008. [2](#)
- [44] Jiachen Li, Jitesh Jain, and Humphrey Shi. Matting anything. *arXiv preprint arXiv:2306.05399*, 2023. [2](#)
- [45] Xiang Li, John Thickstun, Ishaan Gulrajani, Percy S Liang, and Tatsunori B Hashimoto. Diffusion-lm improves controllable text generation. *Advances in Neural Information Processing Systems*, 35:4328–4343, 2022. [3](#)
- [46] Yaoyi Li and Hongtao Lu. Natural image matting via guided contextual attention. In *AAAI*, 2020. [2](#), [4](#), [6](#), [8](#)
- [47] Shanchuan Lin, Andrey Ryabtsev, Soumyadip Sengupta, Brian L Curless, Steven M Seitz, and Ira Kemelmacher-Shlizerman. Real-time high-resolution background matting. In *Proceedings of the IEEE/CVF Conference on Computer Vision and Pattern Recognition*, pages 8762–8771, 2021.
- [48] Shanchuan Lin, Linjie Yang, Imran Saleemi, and Soumyadip Sengupta. Robust high-resolution video matting with temporal guidance. In *Proceedings of the IEEE/CVF Winter Conference on Applications of Computer Vision*, pages 238–247, 2022.
- [49] Tsung-Yi Lin, Michael Maire, Serge Belongie, James Hays, Pietro Perona, Deva Ramanan, Piotr Dollár, and C Lawrence Zitnick. Microsoft coco: Common objects in context. In *Computer Vision–ECCV 2014: 13th European Conference, Zurich, Switzerland, September 6–12, 2014, Proceedings, Part V 13*, pages 740–755. Springer, 2014. [6](#)
- [50] Qinglin Liu, Haozhe Xie, Shengping Zhang, Bineng Zhong, and Rongrong Ji. Long-range feature propagating for natural image matting. In *Proceedings of the 29th ACM International Conference on Multimedia*, pages 526–534, 2021. [2](#)



- [51] Qinglin Liu, Shengping Zhang, Quanling Meng, Ru Li, Bineng Zhong, and Liqiang Nie. Rethinking context aggregation in natural image matting. *arXiv preprint arXiv:2304.01171*, 2023. **2**
- [52] Xihui Liu, Dong Huk Park, Samaneh Azadi, Gong Zhang, Arman Chopikyan, Yuxiao Hu, Humphrey Shi, Anna Rohrbach, and Trevor Darrell. More control for free! image synthesis with semantic diffusion guidance. In *Proceedings of the IEEE/CVF Winter Conference on Applications of Computer Vision*, pages 289–299, 2023. **3**
- [53] Ze Liu, Yutong Lin, Yue Cao, Han Hu, Yixuan Wei, Zheng Zhang, Stephen Lin, and Baining Guo. Swin transformer: Hierarchical vision transformer using shifted windows. In *Proceedings of the IEEE/CVF international conference on computer vision*, pages 10012–10022, 2021. **2, 6**
- [54] Hao Lu, Yutong Dai, Chunhua Shen, and Songcen Xu. Indices matter: Learning to index for deep image matting. In *Proceedings of the IEEE/CVF International Conference on Computer Vision*, pages 3266–3275, 2019. **6**
- [55] Sebastian Lutz, Konstantinos Amplianitis, and Aljosa Smolic. Alphagan: Generative adversarial networks for natural image matting. *arXiv preprint arXiv:1807.10088*, 2018. **1**
- [56] MMEediting Contributors. MMEediting: OpenMMLab image and video editing toolbox. <https://github.com/open-mmlab/mmediting>, 2022.
- [57] Alex Nichol, Prafulla Dhariwal, Aditya Ramesh, Pranav Shyam, Pamela Mishkin, Bob McGrew, Ilya Sutskever, and Mark Chen. Glide: Towards photorealistic image generation and editing with text-guided diffusion models. *arXiv preprint arXiv:2112.10741*, 2021. **3**
- [58] Alexander Quinn Nichol and Prafulla Dhariwal. Improved denoising diffusion probabilistic models. In *International Conference on Machine Learning*, pages 8162–8171. PMLR, 2021. **2, 4**
- [59] Jonas Oppenlaender. The creativity of text-to-image generation. In *Proceedings of the 25th International Academic Mindtrek Conference*, pages 192–202, 2022. **3**
- [60] GyuTae Park, SungJoon Son, JaeYoung Yoo, SeHo Kim, and Nojun Kwak. Matteformer: Transformer-based image matting via prior-tokens. In *Proceedings of the IEEE/CVF Conference on Computer Vision and Pattern Recognition*, pages 11696–11706, 2022. **2, 6, 8**
- [61] Yu Qiao, Yuhao Liu, Xin Yang, Dongsheng Zhou, Mingliang Xu, Qiang Zhang, and Xiaopeng Wei. Attention-guided hierarchical structure aggregation for image matting. In *Proceedings of the IEEE/CVF Conference on Computer Vision and Pattern Recognition*, pages 13676–13685, 2020. **6, 8, 2, 4**
- [62] Aditya Ramesh, Prafulla Dhariwal, Alex Nichol, Casey Chu, and Mark Chen. Hierarchical text-conditional image generation with clip latents, 2022. URL <https://arxiv.org/abs/2204.06125>, 7, 2022. **3**
- [63] Robin Rombach, Andreas Blattmann, Dominik Lorenz, Patrick Esser, and Björn Ommer. High-resolution image synthesis with latent diffusion models. In *Proceedings of the IEEE/CVF conference on computer vision and pattern recognition*, pages 10684–10695, 2022. **3**
- [64] Chitwan Saharia, William Chan, Saurabh Saxena, Lala Li, Jay Whang, Emily L Denton, Kamyar Ghasemipour, Raphael Gontijo Lopes, Burcu Karagol Ayan, Tim Salimans, et al. Photorealistic text-to-image diffusion models with deep language understanding. *Advances in Neural Information Processing Systems*, 35:36479–36494, 2022.
- [65] Chitwan Saharia, Jonathan Ho, William Chan, Tim Salimans, David J Fleet, and Mohammad Norouzi. Image super-resolution via iterative refinement. *IEEE Transactions on Pattern Analysis and Machine Intelligence*, 45(4):4713–4726, 2022.
- [66] Mark Sandler, Andrew Howard, Menglong Zhu, Andrey Zhmoginov, and Liang-Chieh Chen. Mobilenetv2: Inverted residuals and linear bottlenecks. In *Proceedings of the IEEE conference on computer vision and pattern recognition*, pages 4510–4520, 2018.
- [67] Saurabh Saxena, Abhishek Kar, Mohammad Norouzi, and David J Fleet. Monocular depth estimation using diffusion models. *arXiv preprint arXiv:2302.14816*, 2023. **3, 5**
- [68] Arne Schneuing, Yuanqi Du, Charles Harris, Arian Jamasb, Ilia Igashov, Weitao Du, Tom Blundell, Pietro Lió, Carla Gomes, Max Welling, et al. Structure-based drug design with equivariant diffusion models. *arXiv preprint arXiv:2210.13695*, 2022. **3**
- [69] Ehsan Shahrian, Deepu Rajan, Brian Price, and Scott Cohen. Improving image matting using comprehensive sampling sets. In *Proceedings of the IEEE Conference on Computer Vision and Pattern Recognition*, pages 636–643, 2013. **2**
- [70] Jiaming Song, Chenlin Meng, and Stefano Ermon. Denoising diffusion implicit models. *arXiv preprint arXiv:2010.02502*, 2020. **2, 3, 4**
- [71] Yang Song and Stefano Ermon. Generative modeling by estimating gradients of the data distribution. *Advances in neural information processing systems*, 32, 2019. **2**
- [72] Yang Song, Jascha Sohl-Dickstein, Diederik P Kingma, Abhishek Kumar, Stefano Ermon, and Ben Poole. Score-based generative modeling through stochastic differential equations. *arXiv preprint arXiv:2011.13456*, 2020. **3**
- [73] Jian Sun, Jiaya Jia, Chi-Keung Tang, and Heung-Yeung Shum. Poisson matting. In *ACM SIGGRAPH 2004 Papers*, pages 315–321, 2004. **2**
- [74] Yanan Sun, Chi-Keung Tang, and Yu-Wing Tai. Semantic image matting. In *Proceedings of the IEEE/CVF Conference on Computer Vision and Pattern Recognition*, pages 11120–11129, 2021. **2, 6, 8, 4**
- [75] Jingwei Tang, Yagiz Aksoy, Cengiz Oztireli, Markus Gross, and Tunc Ozan Aydin. Learning-based sampling for natural image matting. In *Proceedings of the IEEE/CVF Conference on Computer Vision and Pattern Recognition*, pages 3055–3063, 2019. **1, 6**
- [76] Brian L Trippe, Jason Yim, Doug Tischer, David Baker, Tamara Broderick, Regina Barzilay, and Tommi Jaakkola. Diffusion probabilistic modeling of protein backbones in 3d for the motif-scaffolding problem. *arXiv preprint arXiv:2206.04119*, 2022. **3**
- [77] Ruben Villegas, Mohammad Babaeizadeh, Pieter-Jan Kildermans, Hernan Moraldo, Han Zhang, Mohammad Taghi Saffar, Santiago Castro, Julius Kunze, and Dumitru Erhan. Phenaki: Variable length video generation from open domain

textual description. *arXiv preprint arXiv:2210.02399*, 2022. 3

- [78] Jue Wang and Michael F Cohen. Optimized color sampling for robust matting. In *2007 IEEE Conference on Computer Vision and Pattern Recognition*, pages 1–8. IEEE, 2007. 2
- [79] Wenhai Wang, Enze Xie, Xiang Li, Deng-Ping Fan, Kaitao Song, Ding Liang, Tong Lu, Ping Luo, and Ling Shao. Pyramid vision transformer: A versatile backbone for dense prediction without convolutions. In *Proceedings of the IEEE/CVF international conference on computer vision*, pages 568–578, 2021. 2
- [80] Ning Xu, Brian Price, Scott Cohen, and Thomas Huang. Deep image matting. In *Proceedings of the IEEE conference on computer vision and pattern recognition*, pages 2970–2979, 2017. 1, 6, 8, 2
- [81] Xingqian Xu, Jiayi Guo, Zhangyang Wang, Gao Huang, Irfan Essa, and Humphrey Shi. Prompt-free diffusion: Taking” text” out of text-to-image diffusion models. *arXiv preprint arXiv:2305.16223*, 2023. 3
- [82] Xingqian Xu, Zhangyang Wang, Gong Zhang, Kai Wang, and Humphrey Shi. Versatile diffusion: Text, images and variations all in one diffusion model. In *Proceedings of the IEEE/CVF International Conference on Computer Vision (ICCV)*, 2023. 3
- [83] Jingfeng Yao, Xinggang Wang, Shusheng Yang, and Baoyuan Wang. Vitmatte: Boosting image matting with pretrained plain vision transformers. *arXiv preprint arXiv:2305.15272*, 2023. 2, 4, 5, 6, 8
- [84] Jingfeng Yao, Xinggang Wang, Lang Ye, and Wenyu Liu. Matte anything: Interactive natural image matting with segment anything models. *arXiv preprint arXiv:2306.04121*, 2023. 2
- [85] Haichao Yu, Ning Xu, Zilong Huang, Yuqian Zhou, and Humphrey Shi. High-resolution deep image matting. In *Proceedings of the AAAI Conference on Artificial Intelligence*, volume 35, pages 3217–3224, 2021. 2
- [86] Qihang Yu, Jianming Zhang, He Zhang, Yilin Wang, Zhe Lin, Ning Xu, Yutong Bai, and Alan Yuille. Mask guided matting via progressive refinement network. In *Proceedings of the IEEE/CVF conference on computer vision and pattern recognition*, pages 1154–1163, 2021. 6

## A. Discussions

In our practice, the denoising process from Gaussian noise to clear alpha matte is completed in several DDIM steps. DDIM steps is a specific name for time steps when using the DDIM sampling strategy. Since we use a continuous-time training method, we can arbitrarily specify DDIM steps during inference without retraining the model. After the total number of DDIM steps  $T$  is given during inference, we specify each reverse process in the diffusion process of  $T$  steps as a sampling iteration.

### A.1. DDIM Step

Observing Figure 4 (a), we can see that the performance will increase when the total DDIM steps increase, and Figures 4 (b) and (c) explain the reason for this enhancement: each sampling iteration correct the results. However, this growth tends to be saturated as the number of DDIM steps increases, and performance may even decline after more than 10 steps. We believe that DiffMatte’s ability to correct results comes from continuously exploring the semantic information provided by the encoder and correcting the texture on this basis. At the same time, this iterative process is also supposed to overcome the impact of incorrect predictions in the previous step on subsequent predictions. When the DDIM step size is large, the accumulation of errors can have a negative impact on predictions, causing the model to be unable to maintain its previous performance.

### A.2. Stronger Encoder

As shown in Figure 4 (a), from ResNet-34 to Swin-T to ViT-B, more powerful encoders have brought significant improvements in matting performance. But it’s easy to notice that stronger encoders saturate performance earlier. We believe this is due to the fact that the  $F$  produced by the powerful encoder provides more informative knowledge, allowing the diffusion model to make the most accurate predictions more rapidly. Therefore, further increasing the number of sampling steps does not have a significant improvement effect on diffusion models using powerful encoders. Therefore, it is recommended to use 8 steps of sampling to significantly improve the effect when using a weak encoder. When using a powerful encoder, use sampling within 5 steps to balance computing overhead and performance.

### A.3. Consistent Sampling.

We discussed the negative impact of inconsistent sampling on the diffusion process in the main paper, and give a more intuitive explanation here. We try to use ground truth alpha matte to add noise in each sampling iteration to obtain noise samples during inference to eliminate the impact of previous prediction errors on subsequent predictions and align the sampling during training and inference. In Figure A (a)

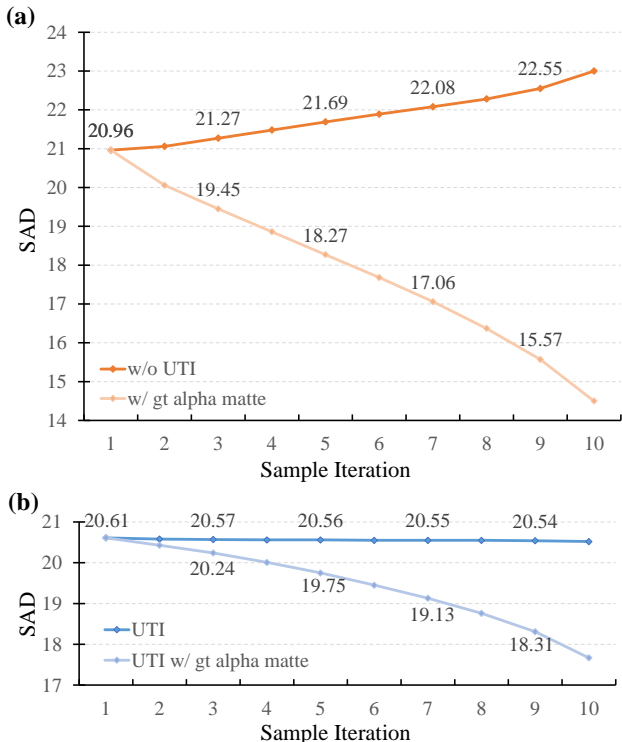


Figure 7. **Consistent Sampling.** Using consistent sampling versus inconsistent sampling. (a) Model without training with UTI. (b) Model training with UTI.

we use the model without UTI self-align, and in Figure A (b) we use the model trained with UTI. We found that using consistent sampling can more obviously improve the accuracy of matting as the number of iterations increases, but because this inconsistency cannot be eradicated, the matting performance of models without UTI decreases. Models using UTI can alleviate the trend of performance degradation to a certain extent, but there is still a big gap in the performance of consistent sampling. At the same time, we found that the model trained using UTI performed worse than the other one with consistent sampling. We believe that UTI training provides the model with resistance to noisy samples, so that it does not rely entirely on previous predictions to get the results of the current iteration.

## B. Decoder Structure Details

The scale of the top-level features of the matting encoder may be  $1/32$  (normal hierarchical backbone network) or  $1/16$  of the input image size (non-hierarchical backbone network or using the Atrous Spatial Pyramid Pooling module). In order to adapt to various matting encoders, we design customized generation rules for the decoder. Given the input channel  $N_c$  and  $N_F$  of  $c$  and  $F$ , we introduce a hyperparameter  $N_d$ , which is a relatively small number, to control the channel numbers of Down-block and Up-block.  $\{N_c, N_d, 2 \times N_d, 4 \times N_d, 4 \times N_d\}$  and  $\{N_F, 8 \times N_d, 8 \times$

Matting Encoder	initial $lr$	epochs	batch size	scheduler value	scheduler milestone	GPUs(A6000)
ResNet-34 [46]	$4e - 4$	150	20	[0.1, 0.05, 0.01]	[30, 90, 140]	2
Swin-Transformer [60]	$4e - 4$	150	20	[0.1, 0.05, 0.01]	[30, 90, 140]	2
ViT-S [83]	$5e - 5$	150	16	[0.1, 0.05]	[30, 90]	2
ViT-S* [83]	$5e - 5$	200	8	[0.1, 0.05, 0.01]	[60, 110, 170]	4
ViT-B [83]	$2.5e - 4$	170	16	[0.1, 0.05, 0.01]	[30, 90, 140]	2

Table 5. Hyperparameters for Adobe Image Matting training. The scheduler value indicates the set of learning rates in different training stages. The scheduler milestone is the set of transition timings (epoch) between stages. \* means using images of size  $1024 \times 1024$  for training.

Matting Encoder	initial $lr$	epochs	batch size	scheduler value	scheduler milestone	GPUs(A6000)
ViT-S [83]	$5e - 5$	150	16	[0.1, 0.05]	[30, 90]	2
ViT-B [83]	$2.5e - 4$	200	16	[0.1, 0.05, 0.01]	[30, 90, 140]	2

Table 6. Hyperparameters for Distinctions-646 training. The scheduler value indicates the set of learning rates in different training stages. The scheduler milestone is the set of transition timings (epoch) between stages.

$N_d, 4 \times N_d, 2 \times N_d, N_d$  are the channel number lists of Down-Block and Up-Block respectively, and an **additional pair of blocks** are stacked when dealing with the feature size of  $1/32$  of the input image. The exchange of texture information between Down-block and Up-block is accomplished by simple feature concatenation. A matting head is added after the last Up-Block to obtain a one-channel alpha matte. The two kinds of blocks additionally incorporate the encoding and fusion of time step information to make our diffusion decoder time-aware. This is achieved by a linear layer that learnably transforms  $t$  values into high-dimensional temporal embeddings  $\tau$ .  $\mathcal{D}$  is constructed only by CNN layers since its role is to refine the texture information during the diffusion process and therefore does not need to use any attention mechanism.

### C. Implementation Details

**Adobe Image Matting.** Following the common practice [19, 60, 80], the training image is cropped to  $512 \times 512$  after synthesizing by random foreground and background, and the corresponding trimap is generated through a dilation-erosion operation using a random kernel size of [1, 30]. We implement our DiffMatte based on several encoders redesigned for matting tasks, including Resnet-34 [46], Swin-Transformer [60], ViT-S and ViT-B [83]. We use the AdamW optimizer for training and incorporate the weight decay trick as well as a multi-stage learning rate adjustment strategy. Notably, to make a fair comparison with [51], we additionally use input images of size  $1024 \times 1024$  for training. Hyperparameters in the training phase vary for models with different settings, which will be explained in Table 5.

**Distinctions-646.** The Distinctions-646 (referred to as D646) dataset provides 646 unique foregrounds and corresponding alpha matte. It is divided into a training set and a test set, which contain 596 training foregrounds and 50 test foregrounds respectively. Data augmentation dur-

Methods	SAD	MSE( $10^3$ )	Grad	Conn
ViTMatte-S [83]	20.57	6.12	10.06	16.97
DiffMatte-ViT(S1)	18.93	5.90	10.17	16.28
DiffMatte-ViT(S10)	<b>18.91</b>	<b>5.81</b>	<b>10.00</b>	<b>16.26</b>
ViTMatte-B [83]	16.22	4.51	7.53	13.56
DiffMatte-ViT(S1)	15.47	4.24	7.18	<b>13.20</b>
DiffMatte-ViT(S10)	<b>15.43</b>	<b>4.21</b>	<b>6.95</b>	13.22

Table 7. Quantitative results on Distinctions-646 [61]. S1 and S10 denote 1 and 10 DDIM time steps.

Methods	SAD	MSE( $10^3$ )	Grad	Conn
AEMatter [51]	17.79	2.39	<b>4.81</b>	12.64
DiffMatte-ViT(S1)	17.16	2.26	5.14	11.42
DiffMatte-ViT(S10)	<b>17.15</b>	<b>2.26</b>	5.13	<b>11.42</b>

Table 8. Quantitative results on Composition-1K [80]. S1 and S10 denote 1 and 10 DDIM time steps.

ing training is consistent with the operation on the Adobe Image Matting dataset. We trained DiffMatte-ViT(S1) and DiffMatte-ViT(S10) on D646, and the training parameter settings are shown in Table 6.

### D. Experimental Results

In Table 7, we provide results on the test set of D646. We compare the performance of DiffMatte-ViT(S1) and DiffMatte-ViT(S10) with ViTMatte-S and ViTMatte-B on official weights trained on the D646 training set. It can be observed that DiffMatte still outperforms ViTMatte under the same backbone. Besides, after training on the D646 training set, DiffMatte adapts to the data domain and can achieve performance improvement as the number of DDIM steps increases, which proves our point in Section 4.5. In Table 8, we present results on large-size training inputs. Our method surpasses AEMatter [51] in most metrics, further demonstrating the effectiveness of our method.



## E. More Visualization Results

Figures 8 and 9 show the comparison of DiffMatte (ViT-B) generalized to D646 and SIMD at 10 DDIM steps with previous state-of-the-art methods. These results show the performance advantages of our approach.

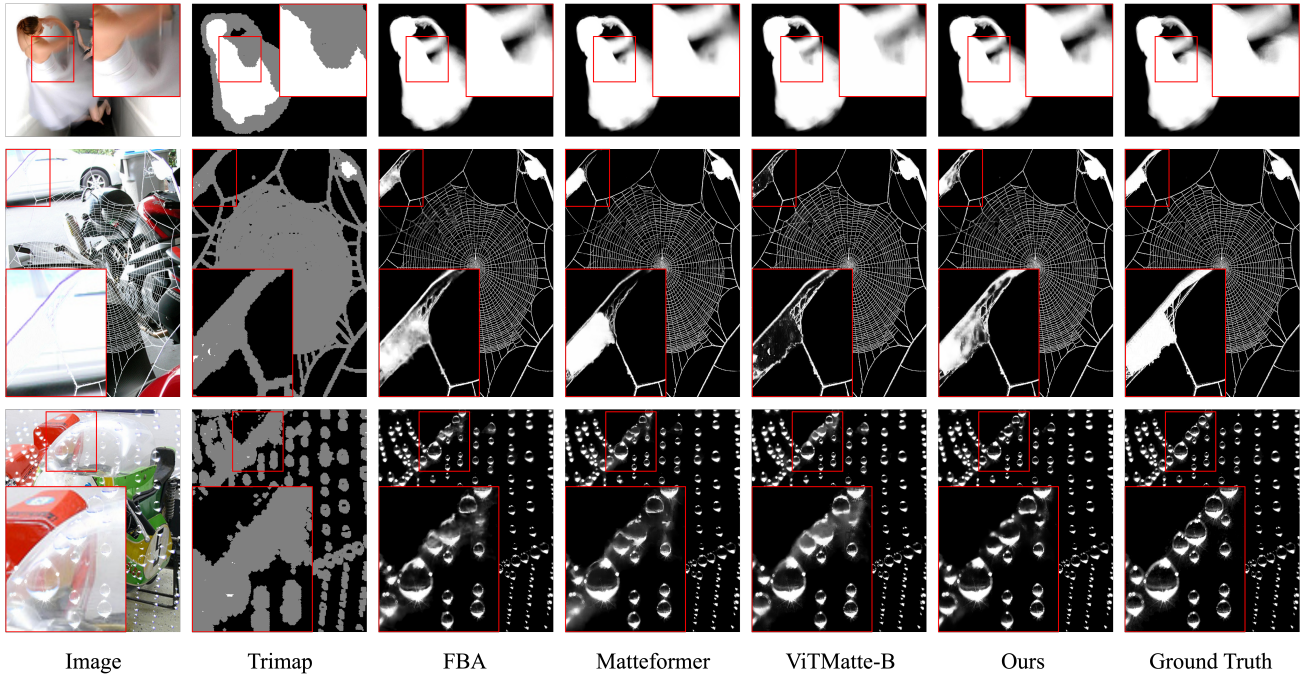


Figure 8. Qualitative generalization results compared with previous SOTA methods on Distinctions-646 test set[61]. Best viewed by zooming in.

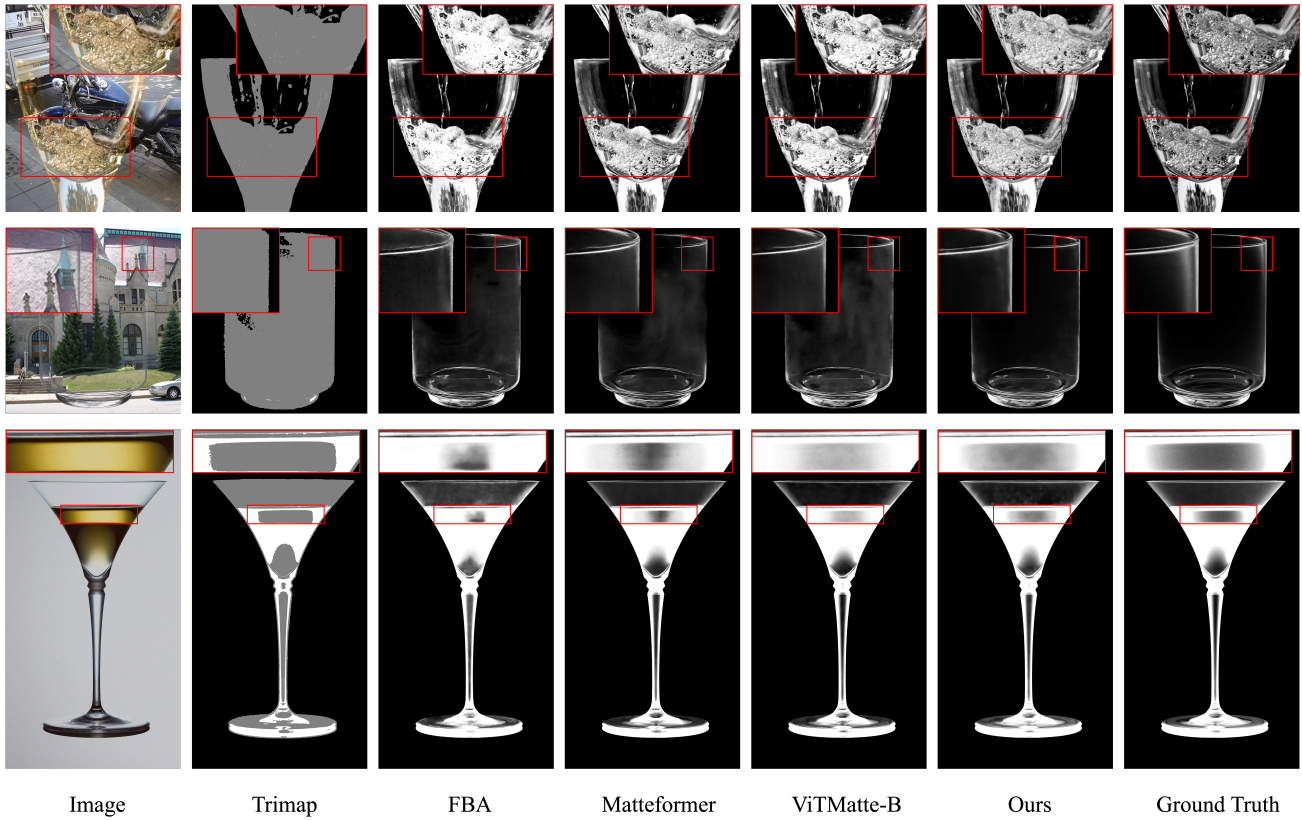


Figure 9. Qualitative generalization results compared with previous SOTA methods on Semantic Image Matting test set [74]. Best viewed by zooming in.